Extraction of the Random Component of Time-Dependent Variability Using Matched Pairs

Ben Kaczer, Jacopo Franco, *Member, IEEE*, Philippe J. Roussel, Guido Groeseneken, *Fellow, IEEE*, Thomas Chiarella, Naoto Horiguchi, and Tibor Grasser, *Senior Member, IEEE*

***Abstract*— Based on the so-called defect-centric statistics, we propose the average impact of a single charged trap on FET threshold voltage as a physically based measure of the random component of time-dependent variability. We show that it can be extracted using matched pairs, analogously to time-zero variability. To that end, the defect-centric statistics of matched pairs are discussed and the correlation between time-zero and time-dependent variances is formalized.**

***Index Terms*— Variability, reliability, FinFETs, matched pairs.**

I. Introduction

As-fabricated, i.e., time-zero variability, both systematic (process-induced) and random, is a well-known phenomenon in deeply-scaled VLSI technologies. For example, the time-zero threshold voltages V_{th0} are assumed to be normally-distributed with mean $\langle V_{th0}\rangle$ and variance ${\sigma_{Vth0}}^2$ [1]. The random component of ${\sigma_{Vth0}}^2$ then scales as

$$ {\sigma_{Vth0,r}}^2 = {A_{Vth}}^2/A_G, \tag{1}$$

where A_{Vth} is a scaling factor and A_G the total channel area [2]–[4]. The index "r" is used to denominate the random component throughout this Letter.

An additional and considerable source of variability in deeply scaled devices arises during operation due to charging of pre-existing and generation of new defects and is manifested as Random Telegraph Noise (RTN) and Bias Temperature Instability (BTI) [5]. We have previously shown that the statistics of this time-dependent variability of threshold voltage shifts ΔV_{th} can be expressed analytically in the so-called *defect-centric model*, which allows to derive a simple but crucial relation between its first two moments $\langle \Delta V_{th}\rangle$ and $\sigma_{\Delta Vth,r}$, namely [5]

$$ {\sigma_{\Delta Vth,r}}^2 = 2\eta\langle \Delta V_{th}\rangle. \tag{2}$$

Manuscript received January 27, 2015; revised February 9, 2015; accepted February 11, 2015. Date of publication February 16, 2015; date of current version March 20, 2015. This work was supported in part by imec's Core Partner Program and in part by the European Commission within the FP7/ICT through the MoRV Project under Grant 619234. The review of this letter was arranged by Editor J. Schmitz.

B. Kaczer, J. Franco, P. J. Roussel, T. Chiarella, and N. Horiguchi are with imec, Leuven 3001, Belgium (e-mail: kaczer@imec.be).

G. Groeseneken is with imec, Leuven 3001, Belgium, and also with the Department of Electrical Engineering, Katholieke Universiteit Leuven, Leuven 3000, Belgium.

T. Grasser is with the Vienna University of Technology, Vienna 1040, Austria.

Color versions of one or more of the figures in this letter are available online at http://ieeexplore.ieee.org.

Digital Object Identifier 10.1109/LED.2015.2404293

Here, η, a device-physics-based parameter with dimension of voltage, represents the *average contribution of a single charged trap* to ΔV_{th}. Since ${\sigma_{\Delta Vth,r}}^2$ increases as the device population ages, we argue that time-dependent variability is best described in terms of η, which to the first order is independent of degradation. Moreover, η scales with channel area as [6]

$$ \eta = B_\eta/A_G, \tag{3}$$

B_η being a scaling parameter. The correct knowledge of B_η, combined with the projection of the expected degradation mean $\langle \Delta V_{th}\rangle$, then allows to make an educated prediction of *degradation distribution in the entire device population of the VLSI application* [5].

Similarly to its time-zero counterpart, time-dependent variability has systematic and random components, which need to be understood separately. Kerber has shown recently that the random component can be extracted using dedicated local 8×8 arrays of FETs, which provide sufficient statistics, while not being affected by systematic effects, and confirming Eq. 3 [4]. Here we demonstrate that, analogously to time-zero analysis [2], standard *matched FET pairs (MPs), widely available in most test-chip layouts, can be used for the same task of extracting random time-dependent variability down to* $\eta \sim 0.1$ *mV range*. We note the impact of hot-carrier stress on device matching has been discussed previously, notably by Magnone *et al.* [7], however, the link with fundamental parameters of time-dependent variability has not been realized.

Here we first describe the statistics of *differential shift* $\delta\Delta V_{th}$ in MPs and confirm through a Monte Carlo simulation that MPs can be used to extract the time-dependent random variability masked by systematic variability. We then apply and validate the proposed analysis technique on real-silicon devices, both n and pFinFETs at different temperatures. Finally, we formalize and briefly discuss the correlation between the correctly-extracted random components of time-zero and time-dependent variabilities.

II. Experimental and Analysis Procedure

We studied both n- and pFinFETs devices with varying channel length L_G and the number of fins N_{FIN}, organized into matched pairs, each pair thus consisting of left "L" and right "R" devices laid out in close proximity. The total channel area of each device is $A_G = (W_{FIN} + 2H_{FIN})L_G N_{FIN}$, where $W_{FIN} + 2H_{FIN} = \sim$60 nm is the total channel width of each fin.

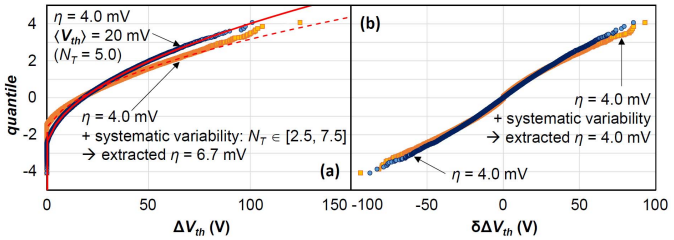

Fig. 1. Probit plots of Monte Carlo simulation of defect-centric distributions in (a) single devices (SD) and (b) matched pairs (MP). Variance and hence η can be readily extracted from the difference $\delta\Delta V_{th}$ distribution obtained on MPs (b). *Additional systematic variability*, generated by distributing the defect density N_T, in single devices (a) *is fully compensated and the original* η *is restored* (b).

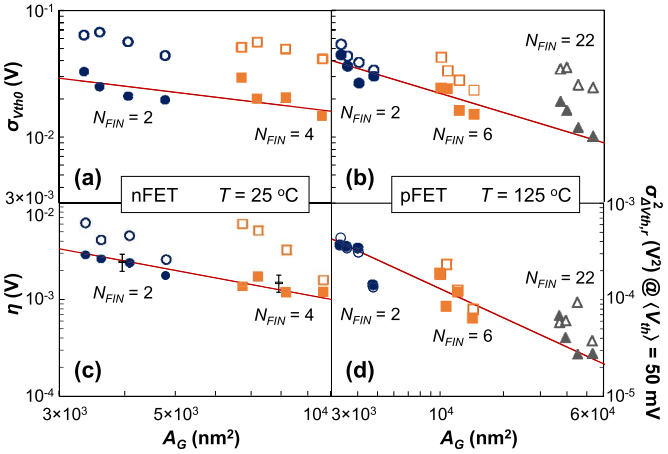

Fig. 2. The random component of both (a)(b) time-zero and (c)(d) time-dependent variabilities, extracted using matched pairs (solid symbols), follow area scaling (Eqs. 1 and 3, lines) in contrast to single devices (open symbols), which are affected by systematic variability. Eq. 2 is used for the right-hand axis. (c) Symbols with error bars (indicating the extraction uncertainty) correspond to η values obtained independently from single-trap discharging event distributions in Fig. 3.

The initial threshold voltage V_{th0} of each device was obtained from the initial I_D-V_G at fixed I_D. Each device was then separately stressed at elevated V_G and low V_D (corresponding to "BTI" stress) for 100 s and the overall threshold voltage *shift* ΔV_{th} was inferred from ΔI_D at ~1 ms after stress [8]. The n- and the pFinFETs were studied at 25 and 125 °C, respectively. Multiple threshold voltage shifts Δv_{th} due to individual defect-discharging events were also extracted from relaxation traces of the nFinFET devices and analyzed separately [5], [9]. Devices showing any abnormality, such as increased gate current or the source and drain currents not equal within a specified margin were disqualified [10]. In total, about 65 device pairs of each size and polarity, distributed over an entire 300 mm wafer, were used for further analysis.

Variances σ^2 of V_{th0} and ΔV_{th}, i.e., ${\sigma_{Vth0}}^2$ and ${\sigma_{\Delta Vth}}^2$, have been calculated by grouping the data in two fashions:

1) "single devices" (SDs), obtained by grouping the respective parameter from *all* ("L" and "R") devices of each size (~130 values in each group), and
2) "matched pairs" (MPs), obtained by grouping the *differences* of the respective parameter of the "L" and "R" devices of each pair of each size (~65 values in each group), i.e.,

$$\delta V_{th0} = V_{th0,L} - V_{th0,R} \tag{4}$$

and

$$\delta\Delta V_{th} = \Delta V_{th,L} - \Delta V_{th,R} \tag{5}$$

Following Refs. [2], [3], i.e., *assuming that the systematic component in closely-spaced "L" and "R" devices is identical*, the variance of the random component is

$${\sigma_{Vth0,r}}^2 = {\sigma_{\delta Vth0}}^2/2 \tag{6}$$

and correspondingly,

$${\sigma_{\Delta Vth,r}}^2 = {\sigma_{\delta\Delta Vth}}^2/2. \tag{7}$$

III. Defect-Centric Statistics of Matched Pairs

A defect-centric distribution describing time-dependent variability is illustrated in Fig. 1a for a particular combination of $\langle\Delta V_{th}\rangle$ and η. This distribution arises from having a Poisson-distributed number n of charged defects in each device (with expectation value N_T) and each defect contributing to ΔV_{th} with an exponentially-distributed shift Δv_{th} (with expectation value η). Consequently, $\langle\Delta V_{th}\rangle = N_T\eta$ [5]. Note the ΔV_{th} distribution in Fig. 1a is highly asymmetric, as only non-negative ΔV_{th} values are expected (for nFET) [5]. When two separate ΔV_{th} values are measured after identical stress of the "L" and "R" devices of a MP population, their difference $\delta\Delta V_{th}$ (Eq. 5) has the distribution illustrated in Fig. 1b. As a consequence of the highly-skewed single-device distribution in Fig. 1a, the distribution of $\delta\Delta V_{th}$ will be in general *non-normal* (see [7], [10]).

We now introduce additional systematic (process-induced) variability, represented by varying the originally constant mean number of defects per device N_T. Each n is thus selected from a Poisson distribution with the expectation value N_T randomly taken from the range indicated in Fig. 1a. This *conceptually* mimics across-wafer variations in gate oxide defect density of traps due process variations, such as plasma-induced damage, or larger degradation in devices with locally thinner oxide. We see that the single-device defect centric distribution is substantially dilated (Fig. 1a). A naive extraction of random variability from this distribution, represented by η, then leads to incorrect conclusions. (Such an error is analogous to obtaining $\sigma_{Vth0,r}$ from single-device time-zero V_{th0} distributions.) When systematic variability in MPs is simulated by using the randomized, but *identical* N_T *for both "L" and "R" devices of each pair*, the MP $\delta\Delta V_{th}$ distribution in Fig. 1b is not significantly changed. When Eqs. 5, 7, and 2 are used, the original value of time-dependent random variability, expressed by η, is duly obtained.

IV. Results, Discussion and Implications

The analysis described above is now applied to real-silicon FinFET devices. From Figs. 2a and b it is apparent that for both wafers tested, the time-zero variances extracted from single devices (open symbols) are affected by systematic variability and thus overestimate the random component extracted from MPs (Eqs. 4 and 6, solid symbols), which follow correct A_G scaling (line, Eq. 1) [2]–[4]. Similarly for time-dependent variability, η obtained on nFinFETs (Fig. 2c)

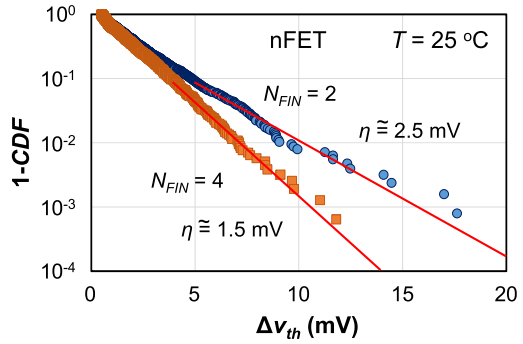

Fig. 3. Distribution of threshold voltage shifts Δv_{th} due to *single* discharging events in nFinFETs. Steps from relaxation traces from four similar areas are combined to boost the tails of both respective distributions.

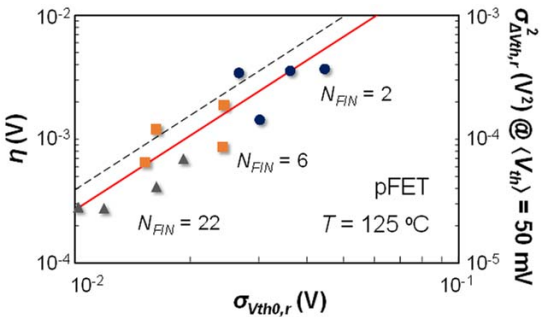

Fig. 4. Correlation between time-zero and time-dependent random variances in the pFinFET devices from Figs 2b and b (solid line, $C \equiv \sim 190$ mV). Correlation for nFinFETs from Figs. 2a and c is given for comparison (dashed line, $C = \sim 130$ mV).

by naive extraction from single devices does not scale correctly with A_G. Thus extracted η overestimates the true value, as illustrated already in Fig. 1. However, when Eqs. 5, 7, and 2 are used, the resulting η'*s* scale excellently with device area and match the intrinsic η values (symbols with error bars in Fig. 2c), extracted independently from its true *physical* origin, i.e., the single trap-discharging event distributions in Fig. 3 [9]. We note that the analysis of individual defect steps is generally a highly elaborate process, involving step detection in relaxation traces with experimental noise, complex "bookkeeping" to avoid double-counting of defects manifesting RTN during the measurement, and the uncertainty in fitting the distribution tail. In contrast, obtaining time-dependent random variability from matched pairs described here is significantly simpler.

The proposed analysis is also applied to pFinFETs (Fig. 2d), where the extraction power of matched pairs becomes apparent at large device areas ($N_{FIN} = 22$), in which η values of the order of 0.1 mV can be extracted without significant effort. Such range is below the resolution of the individual step extraction method (Fig. 3) since the experimental noise levels are $\sim$1 mV in typical high-k gate oxides.

If ${\sigma_{Vth0,r}}^2$ and η (and hence ${\sigma_{\Delta Vth,r}}^2$) are correctly extracted, they will both scale reciprocally with A_G (Eqs. 1 and 3). Only then a correlation between these two quantities, already proposed in [11], can be expected across varying device sizes *within the wafer,* as illustrated in Fig. 4. Furthermore, from Eqs. 1-3 we can easily derive

$$ {\sigma_{\Delta Vth,r}}^2 / {\sigma_{Vth0,r}}^2 = \langle \Delta V_{th} \rangle / C, \tag{8} $$

where

$$ C \equiv {A_{Vth}}^2 / 2B_\eta \tag{9} $$

has dimension of voltage and is an inverse measure of the correlation of the time-zero and the time-dependent *variances*. Note that the correlation of the *variances* does *not* necessarily imply V_{th0} and ΔV_{th} in individual devices are correlated. Eqs. 8 and 9 should help formalize the discussion of time-dependent variability, while the parameter C can be used to study and compare the universality of this dependence across various technologies [2], [11]–[13].

V. Conclusions

We have argued that *time-dependent* random variability, such as due to RTN and BTI, is best characterized by η, the average impact of a single charged trap on ΔV_{th}, and has to be considered in addition to *time-zero* variability. Proper extraction and separation of the components is a prerequisite for understanding of the origins and interplay of both phenomena. Here we have proposed the use of matched pairs as a tool for extracting the random component of *time-dependent* variability.

Acknowledgment

Discussions with Prof. F. Crupi are gratefully acknowledged.

References

[1] T. Mizutani, A. Kumar, and T. Hiramoto, "Analysis of transistor characteristics in distribution tails beyond $\pm 5.4\sigma$ of 11 billion transistors," in *Proc. IEEE IEDM*, Dec. 2013, pp. 33.3.1–33.3.4.

[2] M. J. M. Pelgrom, A. C. J. Duinmaijer, and A. P. G. Welbers, "Matching properties of MOS transistors," *IEEE J. Solid-State Circuits*, vol. 24, no. 5, pp. 1433–1439, Oct. 1989.

[3] C. M. Mezzomo *et al.*, "Characterization and modeling of transistor variability in advanced CMOS technologies," *IEEE Trans. Electron Devices*, vol. 58, no. 8, pp. 2235–2248, Aug. 2011.

[4] A. Kerber, "Methodology for determination of process induced BTI variability in MG/HK CMOS technologies using a novel matrix test structure," *IEEE Electron Device Lett.*, vol. 35, no. 3, pp. 294–296, Mar. 2014.

[5] B. Kaczer *et al.*, "Statistics of multiple trapped charges in the gate oxide of deeply scaled MOSFET devices—Application to NBTI," *IEEE Electron Device Lett.*, vol. 31, no. 5, pp. 411–413, May 2010.

[6] J. Franco *et al.*, "Impact of single charged gate oxide defects on the performance and scaling of nanoscaled FETs," in *Proc. IEEE Int. Rel. Phys. Symp.*, Apr. 2012, pp. 5A.4.1–5A.4.6.

[7] P. Magnone *et al.*, "Impact of hot carriers on nMOSFET variability in 45- and 65-nm CMOS technologies," *IEEE Trans. Electron Devices*, vol. 58, no. 8, pp. 2347–2353, Aug. 2011.

[8] B. Kaczer *et al.*, "Ubiquitous relaxation in BTI stressing—New evaluation and insights," in *Proc. IEEE Int. Rel. Phys. Symp. (IRPS)*, Apr./May 2008, pp. 20–27.

[9] T. Grasser *et al.*, "The time dependent defect spectroscopy (TDDS) for the characterization of the bias temperature instability," in *Proc. IEEE Int. Rel. Phys. Symp. (IRPS)*, May 2010, pp. 16–25.

[10] B. Kaczer *et al.*, "Origins and implications of increased channel hot carrier variability in nFinFETs," in *Proc. IEEE Int. Rel. Phys. Symp. (IRPS)*, to be published.

[11] M. Toledano-Luque *et al.*, "Degradation of time dependent variability due to interface state generation," in *Proc. Symp. VLSI Technol.*, Jun. 2013, pp. T190–T191.

[12] R. Hussin *et al.*, "Interplay between statistical variability and reliability in contemporary pMOSFETs: Measurements versus simulations," *IEEE Trans. Electron Devices*, vol. 61, no. 9, pp. 3265–3273, Sep. 2014.

[13] D. Angot *et al.*, "BTI variability fundamental understandings and impact on digital logic by the use of extensive dataset," in *Proc. IEEE IEDM*, Dec. 2013, pp. 15.4.1–15.4.4.